SANDIA REPORT
SAND2014-4308
Unlimited Release
Printed June 2014

Prompt Radiation-Induced Conductivity in Polyurethane Foam and Glass Microballoons

E.F Hartman, E F Preston, T. A. Zarick, and T. J. Sheridan

Prepared by
Sandia National Laboratories
Albuquerque, New Mexico 87185 and Livermore, California 94550

Sandia National Laboratories is a multi-program laboratory managed and operated by Sandia Corporation, a wholly owned subsidiary of Lockheed Martin Corporation, for the U.S. Department of Energy's National Nuclear Security Administration under contract DE-AC04-94AL85000.

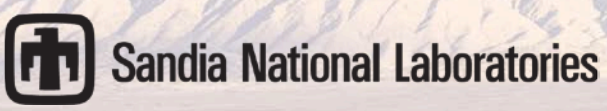

Issued by Sandia National Laboratories, operated for the United States Department of Energy by Sandia Corporation.

Available to DOE and DOE contractors from
U.S. Department of Energy
Office of Scientific and Technical Information
P.O. Box 62
Oak Ridge, TN 37831

Telephone: (865) 576-8401
Facsimile: (865) 576-5728
E-Mail: reports@adonis.osti.gov
Online ordering: http://www.osti.gov/bridge

Available to the public from
U.S. Department of Commerce
National Technical Information Service
5285 Port Royal Rd.
Springfield, VA 22161

Telephone: (800) 553-6847
Facsimile: (703) 605-6900
E-Mail: orders@ntis.fedworld.gov
Online order: http://www.ntis.gov/help/ordermethods.asp?loc=7-4-0#online

SAND2014-4308
Unlimited Release
Printed June 2014

Prompt Radiation-Induced Conductivity in Polyurethane Foam and Glass Microballoons

E.F Hartman, T. A. Zarick, T. J. Sheridan
Radiation Effects Experimentation
Sandia National Laboratories
P. O. Box 5800
Albuquerque, New Mexico 87185-MS1167

E. Preston
ITT Exelis Mission Systems
655 Space Center Drive
Colorado Springs, CO 80915-3604

Abstract

We performed measurements and analyses of the prompt radiation-induced conductivity (RIC) in thin samples of polyurethane foam and glass microballoon foam at the Little Mountain Medusa LINAC facility in Ogden, UT. The RIC coefficient was non-linear with dose rate for polyurethane foam; however, typical values at 1E11 rad(si)/s dose rate was measured as 0.8E-11 mho/m/rad/s for 5 lb./cu ft. foam and 0.3E-11 mho/m/rad/s for 10 lb./cu ft. density polyurethane foam. For encapsulated glass microballoons (GMB) the RIC coefficient was approximately 1E-15 mho/m/rad/s and was not a strong function of dose rate.

ACKNOWLEDGMENTS

The authors acknowledge the excellent support of the Boeing employees at the Little Mountain LINAC Facility near Ogden, UT.

TABLE OF CONTENTS

FIGURES

NOMENCLATURE

Abbreviation	Definition
GMB	glass microballon
RIC	radiation-induced conductivity
STP	Standard temperature and pressure
PCD	Photo conducting device
TLD	Thermo luminescent dosimeter

1. INTRODUCTION

We performed radiation-induced conductivity (RIC) experiments on three different types of foam samples. The samples types were 5 lb. polyurethane foam, 10 lb. polyurethane foam, and 828 glass microballoon. Most samples were 3mm thick. A description of how the experiments were performed and the radiation test source are provided later in this report after a discussion of test results.

The two polyurethane foams were closed cell with CO2 as a blowing agent. Estimates for typical cell size diameter in the polyurethane foams are 600-800 microns for the 5 lb. foam and 400-600 for the 10 lb. foam. Cell sizes are variable within the foam. One also has to consider that there will be some gas diffusion through the resin walls of the foam, so the composition of the gas may vary with time and location in the foam. Note that foams typically have an outer skin that is more dense and rigid than the interior foam. The electrical properties of foams can be different if this skin is removed.

GMB (D32/4500) particle size for the glass balloons is about 50 microns. The balloons are borosilicate glass filled by mostly sulfur dioxide. The epoxy is typically EPON 828 resin cured with diethanolamine curing agent. The epoxy makes up about 52% of the volume.

For each experiment there is only a single RIC cell with a biased electrode with guard rings on one side and ground metal contact on the other side of the foam sample. The samples, though fairly thin, are reasonably thick compared to most of the gas-filled bubbles or gas-filled glass balloons.

2. TEST SUMMARY POLYURETHANE FOAM

For the polyurethane closed cell foam, there are solid cell wall portions with rather low radiation-induced conductivity within that portion, and also gas bubble cells with mainly CO2 gas that have a much higher RIC coefficient than the solid portion. There are also capacitances that differ for the solid and gas portions. In fact, the gas-filled part of the foam has a conductivity or RIC coefficient that is several orders of magnitude higher than the solid portion. Still the foam cannot be modeled as only a conducting gas as the solid portions intervene.

It is also evident for polyurethane foam, that stored charge within the foam is an issue to be considered when testing. For example as shown in Figure 1, with a bias of 100V across the 5 lb./cu ft. polyurethane foam sample, the foam conductivity response results in a first shot measured voltage across 50 ohms of much larger magnitude than subsequent radiation exposures (or shots) produce. Each shot contains a series of 50 ns radiation pulses. Each consecutive pulse shows a smaller response, both for biased and unbiased shots. Figure 1 shows raw data of the RIC response over a train of pulses with the pulses coming to a more common value only after 10 or more pulses.

As shown in Figure 2, for zero bias across the same sample, the data tends toward zero, but the first signal is nearly as high as the first biased signal, with opposite polarity. There appears to be a significant amount of stored charge from the previous shots. The ability of dielectric foams to store charge on the inner surfaces of voids is

well known from the study of ferroelectrets (1). The name comes from ferromagnetic like hysteresis behavior, as the polarization of the voids may flip by applying an external field when the breakdown strength of the gas is reached. In their charged state, ferroelectrets will have piezoelectric properties. The pattern is similar for cells biased in the opposite direction:

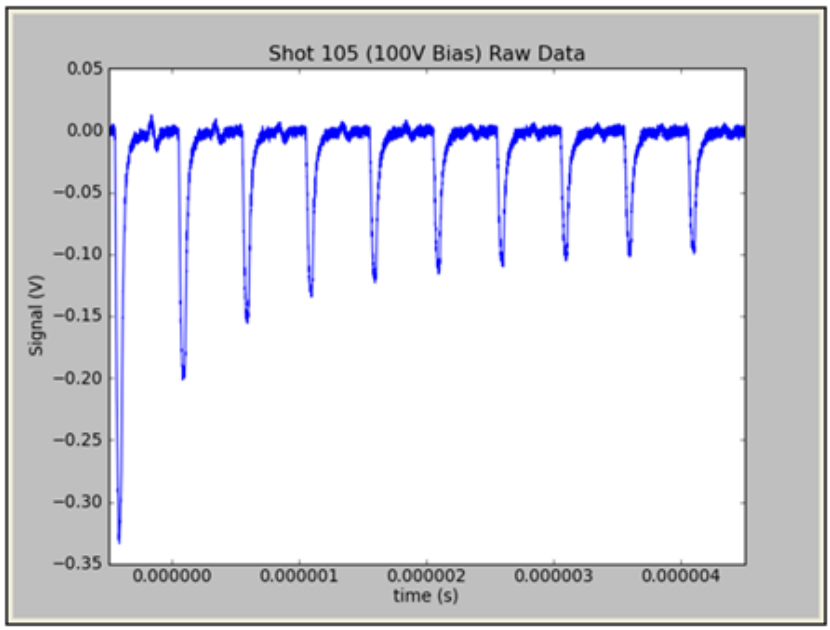

Figure 1. Raw data of the RIC response for biased 5 lb. polyurethane foam

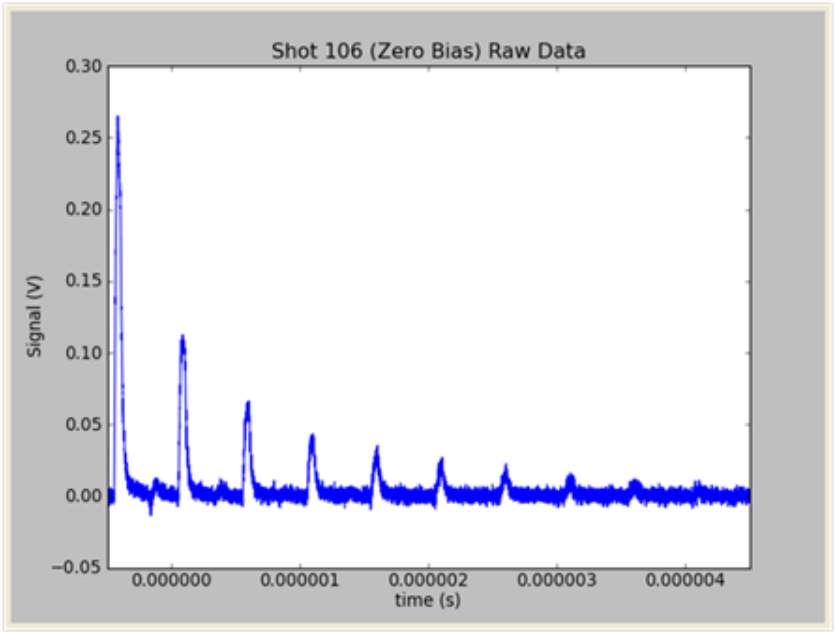

Figure 2. Raw data of the RIC response for unbiased 5 lb. polyurethane foam

For a negatively biased sample, similar responses for RIC appear but of opposite polarity, and the zero bias shots used to clear the sample before changing the bias

polarity also are similar though of opposite polarity to the test conditions of negative polarity bias. This is shown in Figure 3 and Figure 4, respectively.

The responses appear symmetric with opposite bias. Clearing shots were performed between each biased shot, so the first pulse in the train should give a good measure of the actual prompt RIC. However, the responses are complex.

Assuming the clearing shots are successful at eliminating stored charge, only the first pulse in a train will exhibit the untainted prompt RIC. Only these pulses are used in subsequent analysis. However, examining Figure 3 shows there is a substantial buildup of stored charge even during the first pulse. The response of the second pulse is little more than half that of the first. The stored charge must be generating a substantial cancelling field within the material.

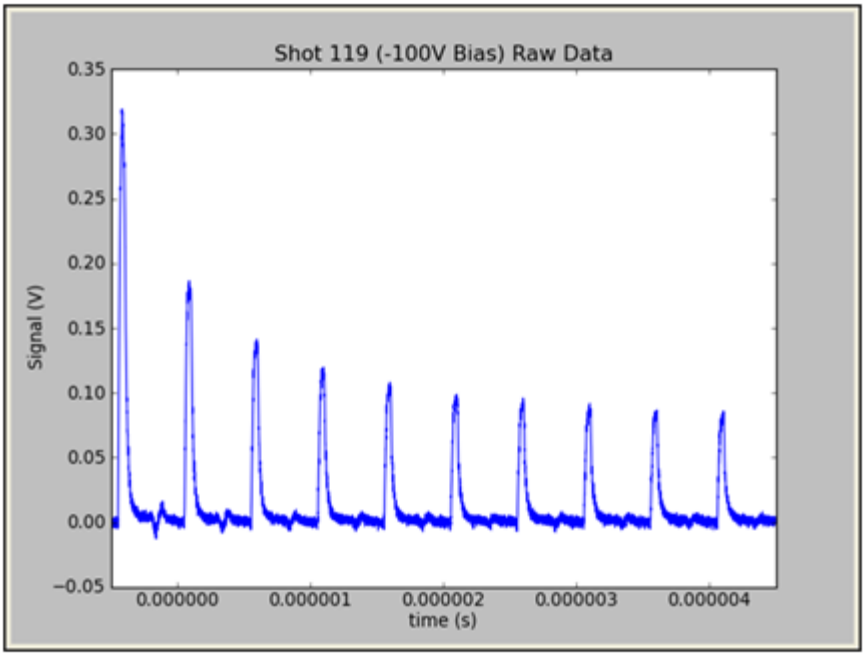

Figure 3. Raw data of the RIC response of 5 lb. polyurethane foam with negative bias applied

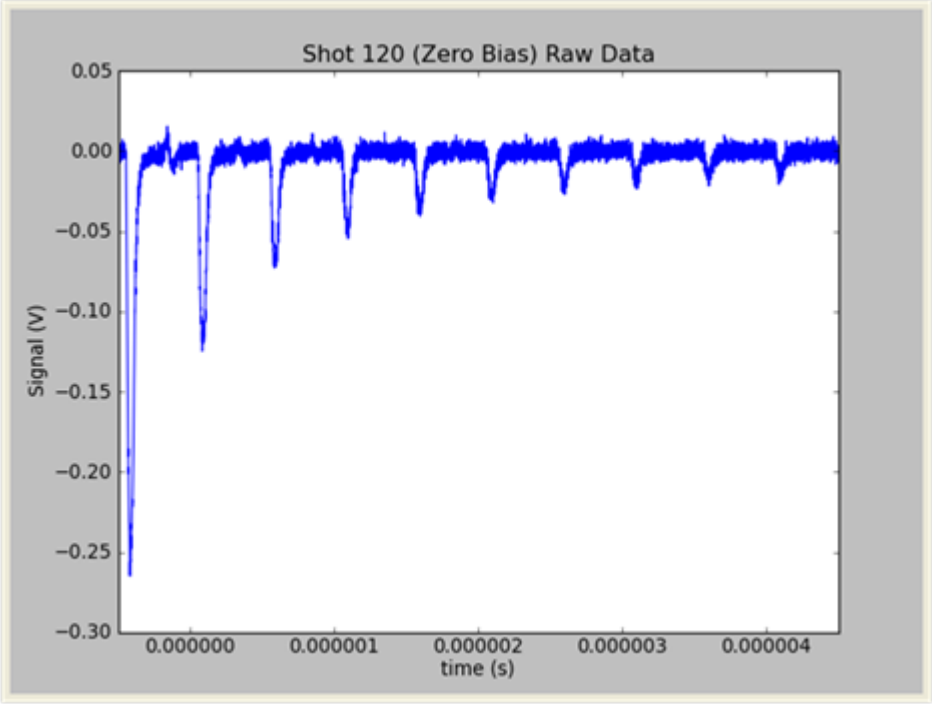

Figure 4. Raw data of the RIC response of 5 lb. polyurethane sample at zero bias that was previously irradiated

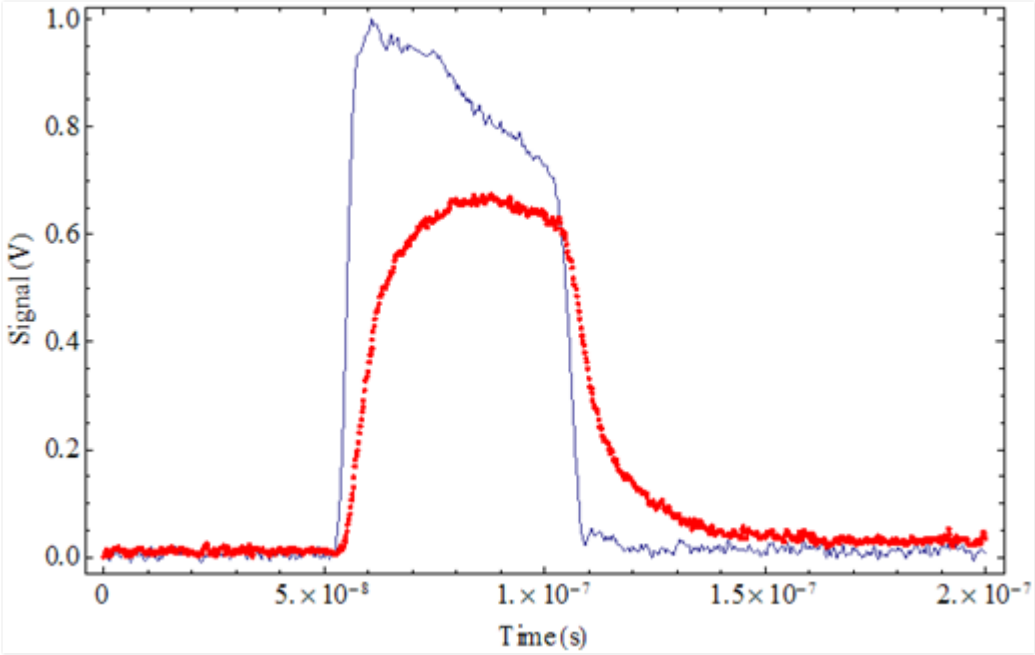

Figure 5. First waveform

Figure 5 shows the first waveform (red) from a shot on 5 lb./cu ft. polyurethane foam biased to +1000V, superimposed with a normalized PCD signal (blue) of the radiation time history.

This signal exhibits a significant rise time and delayed conductivity. If the RIC is dominated by the gas conductivity, then it should either closely follow the pulse or quickly quench due to field exclusion. This response appears somewhat like the radiation response of a solid (2-9), with a characteristic rise time, equilibration, and decay. There is a slight drop in the signal before the end of the pulse, but this may be due to the pulse shape. Letting the normalized PCD waveform be, we can fit the response with an exponential rise

$$V(t) = k\Theta(t - t_0)\left(1 - e^{-(t-t_0)/\tau}\right) f(t) \qquad (1.1)$$

where $\Theta(x)$ is the Heavyside step function. The result of this fit on shot 113 is shown in Figure 6.

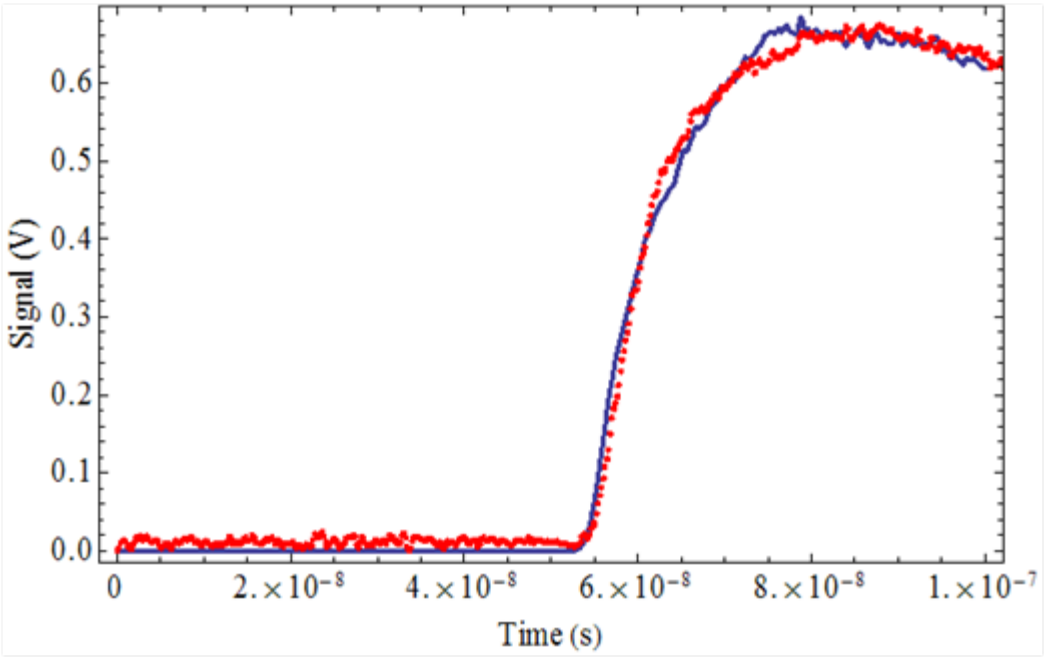

Figure 6. The rise portion of shot 113 (red), with a functional fit (blue). The time constant is 14 ns.

We don't expect the rise to be purely exponential, but to contain several components with different time constants, so the fit is reasonable. More importantly, this shows that the drop toward the end of the pulse is explained by the electron pulse shape, and not due to field exclusion.

However, we are left with a conundrum: if the stored charge is building during the pulse, than it should be reducing the internal field in proportion, and we should see a decline in the conduction current during the pulse. The fact that subsequent pulses in the train show reduced conduction currents demonstrates that this internal field continues to build with added dose, up to some saturation level.

But then why doesn't the second pulse in Figure 3 start with a conductivity where the first one left off? Perhaps the stored charge is mostly generated *between* pulses, where the conductivity is rapidly dropping but charge is still moving due to the external field. During the pulse, the higher conductivity will prevent significant electric fields from forming. This doesn't, however, explain why the stored charge doesn't then discharge during subsequent pulses.

A fit to the decay of the delayed RIC for shot number 113, yields a time constant of about 8.5 ns. The fit is shown in Figure 7.

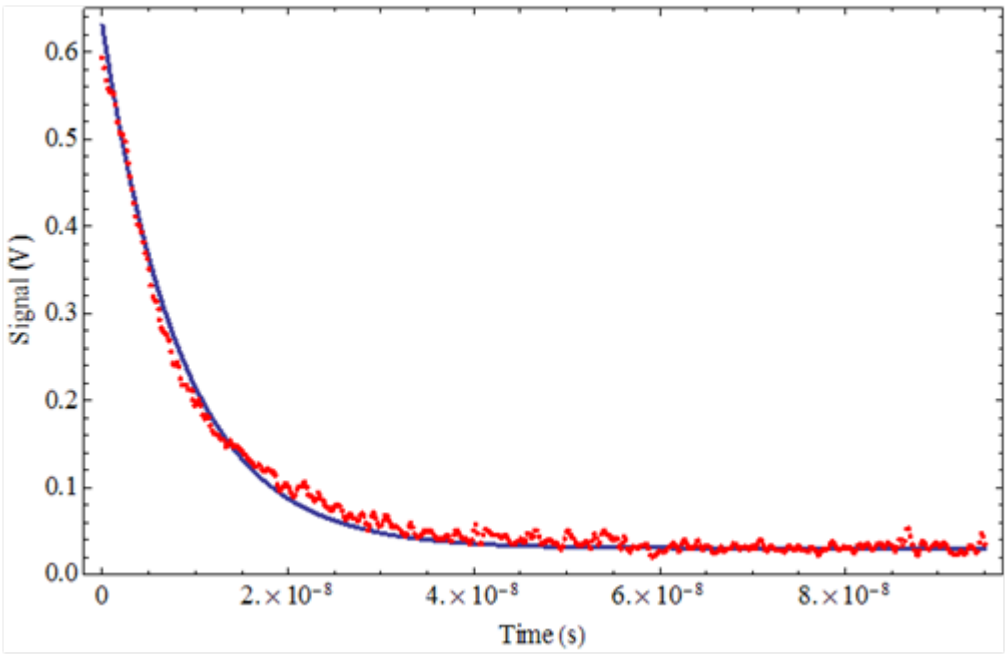

Figure 7. Decay time response plot

The theory of Simpson (10) predicts the same time constants for equilibration and decay, but this is of course only a notional model based on the existence of conduction bands and traps. As emphasized elsewhere, these are only analogous constructs, since there are no Bloch states in a disordered solid like the polymer resin used in the foam. The presence of reasonable well-defined equilibration and decay time show that the foam essentially acts like a solid. This is likely because the field is rapidly excluded from the gas regions, and the observed conductivity is due to transport across the resin or polymer skeleton portion of the foam.

The experimental results for the 5 lb./cu ft. polyurethane foam are shown below in Figure 8. There is a large discontinuity across zero bias. This is an inherent nonlinearity of the RIC, rather than an artifact of the delayed conductivity as have been seen in solid dielectric RIC measurements. Direct drive caused by the electron beam is not important on these high conductivity scales. Thus, the zero bias data point can be taken to be essentially zero. The conductivity is nonlinear with bias. While this can happen for a few solid dielectrics, most solid dielectrics are linear with bias during RIC measurements. The non-linear response is present in all the Polyurethane foam data for both 5 lb. and 10 lb. foam.

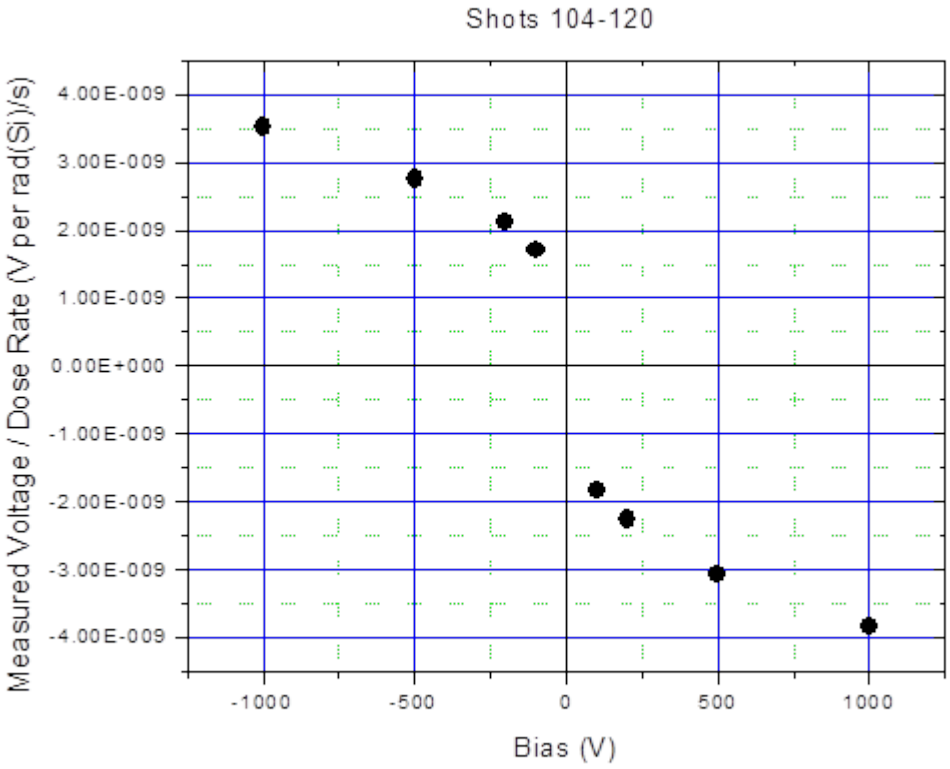

Figure 8. Measured voltage/ dose rate vs. bias voltage (V) for 5 lb./cu ft. foam

A fractional power law is a very good fit for the data, as seen in Figure 9.

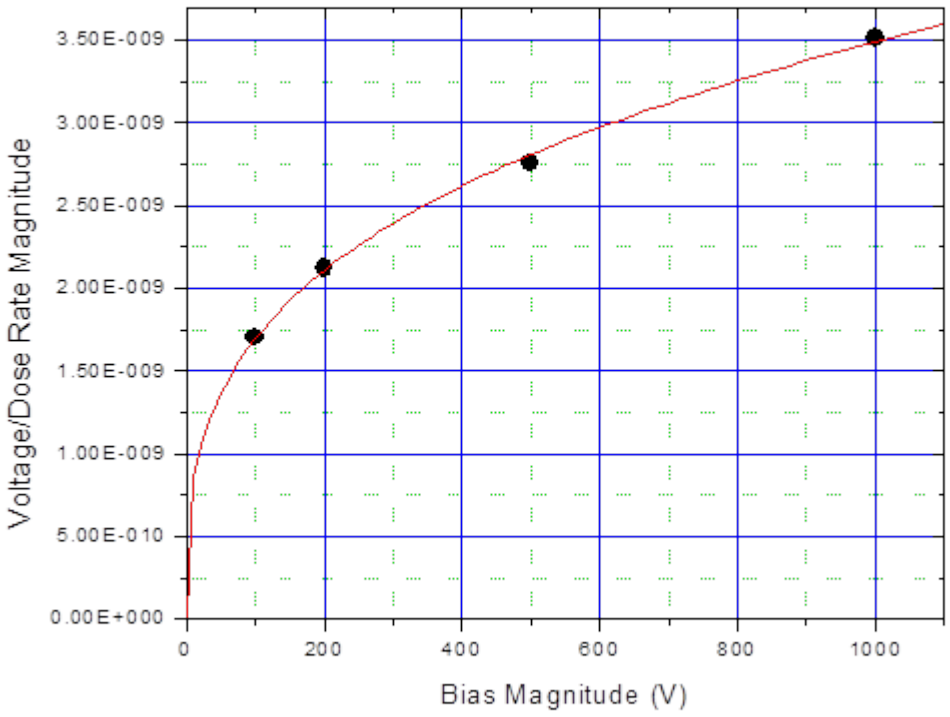

Figure 9. Fractional Power Law Fit for the Positive bias data of shots 104-120 for 5 lb. foam

The parameter errors for the fit are only 1% to 2%. Since they involve fractional powers, we need to use absolute values of bias and measured voltage to avoid imaginary numbers. For simplicity, the positive and negative bias parts are fit separately. The parameters come out nearly identical, indicating very good symmetry with bias, supporting the assumption that direct drive is not important.

As with the other RIC experimental data, we divide the measured voltage by the dose rate of each shot, to remove slight shot to shot variations. This assumes the response is linear with dose rate in the narrow range of a single series of shots. After the parameter fit, we then multiply the coefficient by the average dose rate of the series.

In the fits, the scope voltage V_S is related to the bias voltage V_B with a power law

$$V_S = -aV_B^b \qquad (1.2)$$

The coefficient *a* in equation (1.2) will have units of V^{1-b} . It can be odd dealing with fractional powers of a quantity with units, so an easier way might be to introduce a potential scale V_0 so that

$$V_S = -a' V_0 \left(\frac{V_B}{V_0} \right)^b \tag{1.3}$$

and $a = a' V_0^{1-b}$. In the following analysis, we use form (1.2), since the choice of V_0 is arbitrary, but (1.3) will be easier if one has to change units.

The basic measurement circuit relation, ignoring direct drive, can be written

$$V_S = -\frac{R_S V_B}{R_{ric}} \tag{1.4}$$

This assumes R_{ric} is much larger than the parasitic resistances in the measurement circuit, so they can be ignored. With the definition $R_{ric} = \frac{d}{A\sigma_{ric}}$ we get

$$\sigma_{ric} = \frac{ad}{R_S A} V^{b-1} \tag{1.5}$$

Note that since $b < 1$, the conductivity is a decreasing function of the bias, as we expect from the behavior of Figure 8. This also means that the conductivity diverges as the bias voltage goes to zero. This may seem awkward, but the current will remain finite, since $J = \sigma E \sim E^b$. In terms of electric field, the conductivity is

$$\sigma_{ric} = \frac{ad^b}{R_S A} E^{b-1} \tag{1.6}$$

We would prefer that the conductivity depend only on dose rate and the electric field. However, since in (1.6) it depends on the fractional power of *d*, the sample thickness, it is not independent of the experimental parameters. This scaling is implied by the power law nature (1.2), and it is a very good fit. This implies that the resistance, which would normally scale linearly with the thickness, also scales as d^b.

The dependence on the foam thickness *d* may represent an effective percolation length across the sample. That is, as the foam gets thicker, there are more paths for conduction through the solid, therefore the resistance increases more slowly with thickness than one would expect. Basically, the scaling is the result of a current percolation problem. The exponent *b* will depend on connectivity properties of the solid matrix.

The *volume* of matrix material vs. voids is proportional. So if we just removed the voids in the sample, the thickness decreases. The density of solid polyurethane would be 65 lb./ft3, so the 5# and 10# foams are only 7.7% and 15% matrix material by volume.

The parameters *a* and *b* in (1.2) have a behavior that is well defined with dose rate. They can also be modeled with power laws, though not quite as well as the V_S/V_B relation.

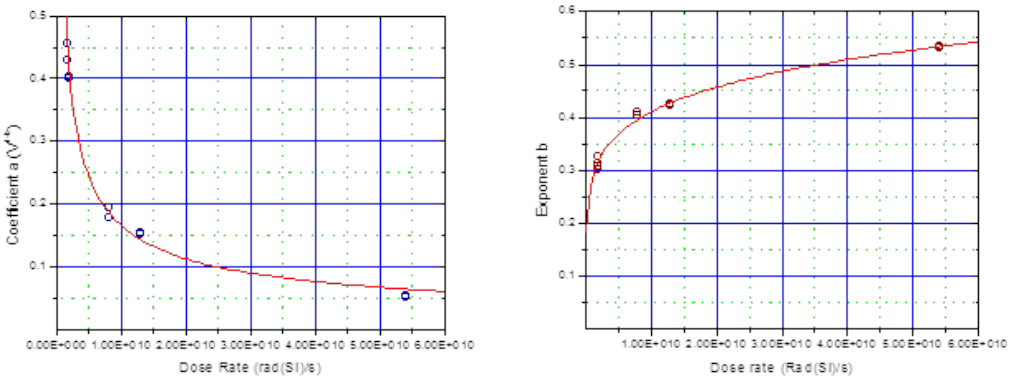

Figure 10. The coefficient a and exponent b from expression (1.1) as they depend on dose rate with power law fits

Table 1 Coefficients and Exponents

parameter	coefficient (Rad(Si)/s)$^{-exponent}$	exponent
a (V^{1-b})	5.8240E-5	0.5547
b (unit less)	0.01123	0.15626

For instance,

$$a(\dot{D}) = 58240\dot{D}^{0.5547}\frac{V^{1-b}}{\left(Rad(Si)/s\right)^{0.5547}} \qquad (1.7)$$

The same approach for 10 lb./cu ft. polyurethane foam yields the following parameters:

Table 2 Parameter Values

parameter	constant	coefficient (Rad(Si)/s)$^{-exponent}$	exponent
a (V^{1-b})	-5.765E-11	3.152E-5	0.51932
b (unit less)		0.0024	0.221109

In this case, the power law fit for these parameters is not as clean. The coefficient, in particular, requires the addition of a constant to look reasonable. Being a negative constant, this will limit its applicability to very high dose rates.

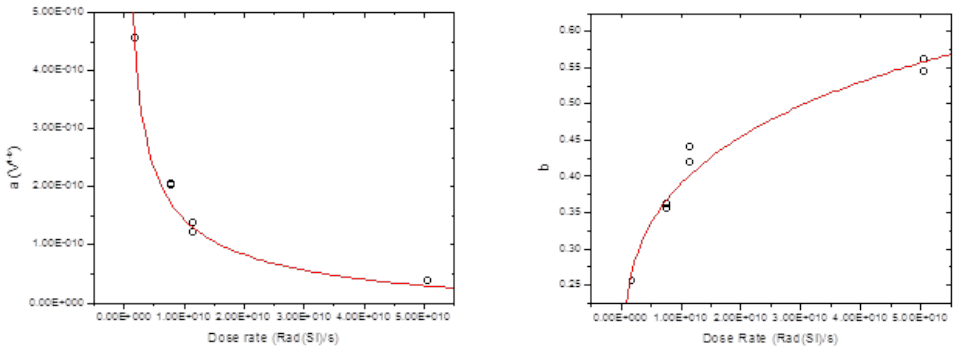

Figure 11. Plots of power law parameter fits for a and b as a function of dose rate in 10 lb./cu ft. polyurethane foam

The next Figure 12 shows the conductivity of 5 lb. polyurethane foam as a function of the electric field based on the power law models for increasing dose rates bottom to top of figure.

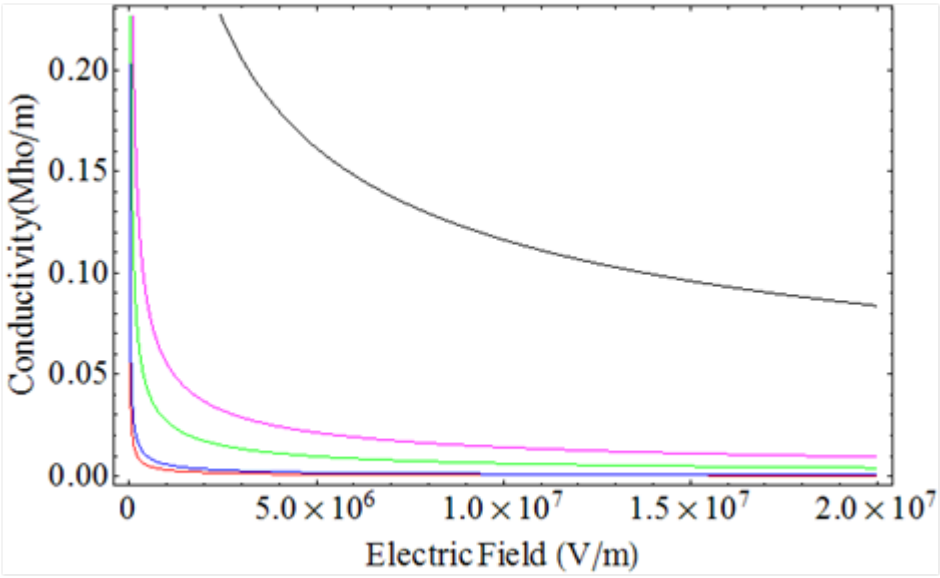

Figure 12. Plots of power law parameter fits for a and b as a function of dose rate in 10 lb./cu ft. polyurethane foam

The following figure compares the conductivity of 5 lb. polyurethane foam with 10 lb. polyurethane foam as a function of dose rate while holding the electric field at 1 MV/m.

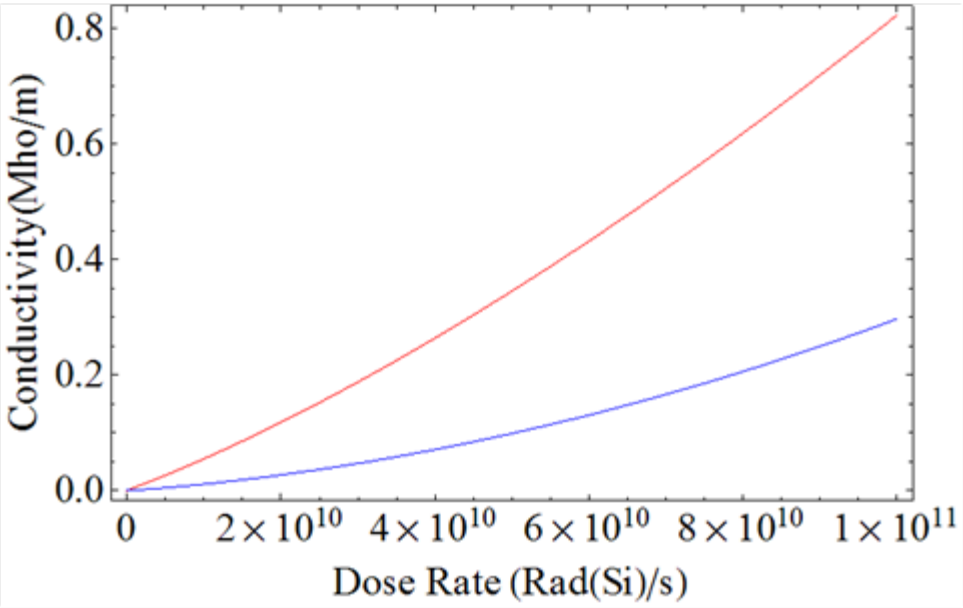

Figure 13. The conductivity of 5 lb. and 10 lb. polyurethane foam vs. dose rate for E = 1MV/m

2.1. Physical Model

According to an Adept simulation, with a 19.154 MeV average linac source electron energy, the deposition in standard temperature and pressure CO2 (n=2.547E+25 m^{-1}) is 2.0648 mev-cm2/g, whereas in silicon the dose would be 2.1584 mev-cm2/g. We will use a ratio of 0.96 in converting doses per unit mass.

Consider a shot of high dose, 6000 Rad(Si). We can't find specific ionization efficiency data for carbon dioxide, but it's probably safe to assume it's similar to O2 or N2, in the range of 30-35 eV/ion pair. But this is the total ionization efficiency, and there is a lag in the formation for secondary electrons. However, the energy collision cross sections for electrons with CO2 are sufficiently high that we expect electrons to be thermalized in less than a nanosecond.

The 6000 Rad(Si) translates into a dose of 4.38E+10 eV in a 500 micron diameter void filled with a CO2 at STP. If we assume all this charge is deposited on the surface of the bubble, it yields a surface charge density of 2.97E-4 C/m2. Taking this divided by the vacuum permittivity to give the scale of the electric fields in the bubble, we get about 33 MV/m. This is an order of magnitude greater than the largest externally applied field, so we can conclude that there is enough gas ionization to quench the fields inside the bubbles during the experiment. The large stored charge observed in subsequent shots supports this notion. However, if we take the data from Figure 5 as typical, the RIC resistance is still more than 80 kilo Ohm, so we are not seeing a collapse of the electric field across the foam. Most of the electric field must be supported across the solid polymer, and the RIC conductivity will actively bleed off the charge on the void surfaces.

A previous SPHINX experiment (11) used much shorter pulse widths, between 2.5 and 10 ns. The observed exponential quench of the RIC current was found to be

consistent with a gas-only conduction model. However, the data are not overlaid with PCD's, so it's difficult to verify this interpretation. The exponential drop could be delayed RIC rather than field exclusion. The agreement with the gas mobility model is impressive, but in these more recent experiments reported here, we do not see a reduction in the RIC signal until well into the 50 ns pulse, and it is modest. There is a build-up of the signal for the first 30 or 40 ns, which is difficult to reconcile with the SPHINX interpretation.

It may be that the field is rapidly excluded from the voids, and we are seeing a signal only from the RIC of the resin. RIC in the resin matrix would be enhanced by the local electric fields from charge deposition. Another way to think of it is the E-field is applied over an effectively smaller thickness of material due to the voids.

The actual conduction through the sample probably consists of charge neutralization across barriers of the matrix materials. The electric field through the resin will be enhanced by the ratio of the void size to the resin thickness, probably an order of magnitude. However, since the electric field in the resin will depend on the pore size, the conduction through the resin or polyurethane solid matrix will vary with the pore size distribution. Walls between large voids will have to bear an enormously multiplied field, and will conduct rather easily. This conduction will neutralize surface charges and allow current to flow through the gas. Small voids will act as a relative barrier to conduction. The power law for effective thickness may be the result of a percolation-like problem. Additionally, the internal field due to the stored charge will act to counter some of the applied bias.

2.2. Glass Micro-balloon

The data from the glass microballoon material behaves even more like a solid dielectric in contrast to the polyurethane foam previously discussed. Very similar results are seen during the train of electron beam pulses, with only slight build-up of stored charge apparent. The zero bias shots show distinct direct drive levels.

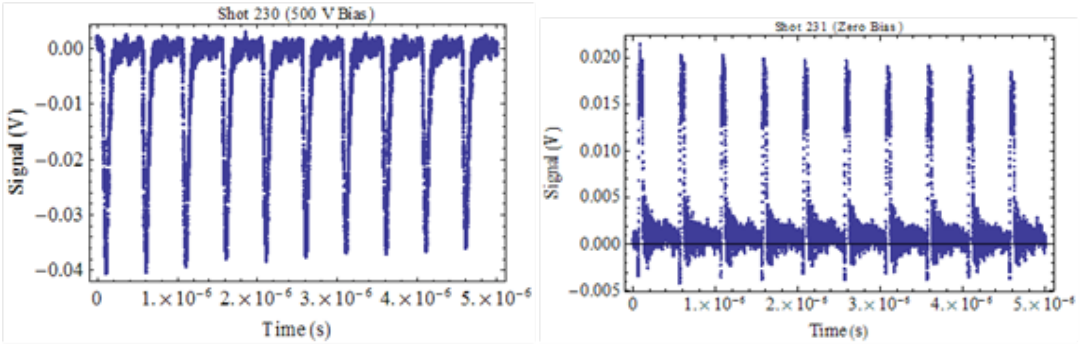

Figure 14. Signal pulse trains GMB shots 230 series (500V) and next zero bias shot series 231 (0V)

Notice that the zero bias signals have about half the magnitude of the 500 V bias signal, and much like in solid dielectrics, the direct drive is substantial from the Linac electron beam.

If we zoom in on the first pulse, we see a signal with a continuous build-up and long decay (Figure 15). This looks similar to the solid Kapton data (2), where current equilibrium was not reached in 50 ns. Since all GMB shots were conducted with a 50 ns pulse width, we can't fully characterize GMB RIC from this data. However, we can derive a RIC coefficient that will be valid for this pulse width, and we can probably scale this linearly to shorter pulses with reasonable accuracy.

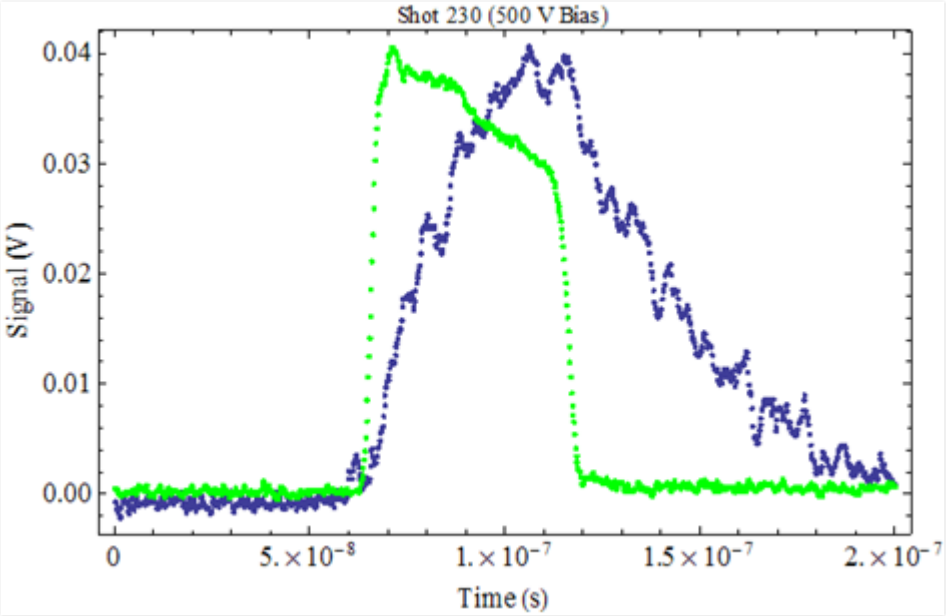

Figure 15. Shot 230 RIC signal (blue) superimposed with the re-scaled PCD radiation time history signal

The results from a typical series of shots (240-252) are shown in Figure 16. There does appear to be a slight amount of nonlinearity, but the response seems pretty flat beyond V. The response is also clearly shifted upwards slightly by the current contribution of the linac beam produced direct drive. We can avoid the complexity of fitting to power laws here by fitting the slopes of positive and negative bias independently, ignoring the zero bias data point. This gives an effective RIC coefficient as shown in Table 2.

Table 2. RIC Coefficient

Shots	Average Dose rate (rad-Si/s)	RIC coefficient
225-239	1.77E+9	1.24E-15
240-252	7.37E+9	9.17E-16
253-257	4.74E+10	4.34E-16
268-284	1.11E+11	1.53E-15

The results of the shot series 253-257 were poor, and should probably be excluded. Without that point on the graph in Figure 16, the conductivity vs. dose rate is best represented with a linear fit, with a coefficient of 1.25E-15 Mho/m per rad(Si)/s.

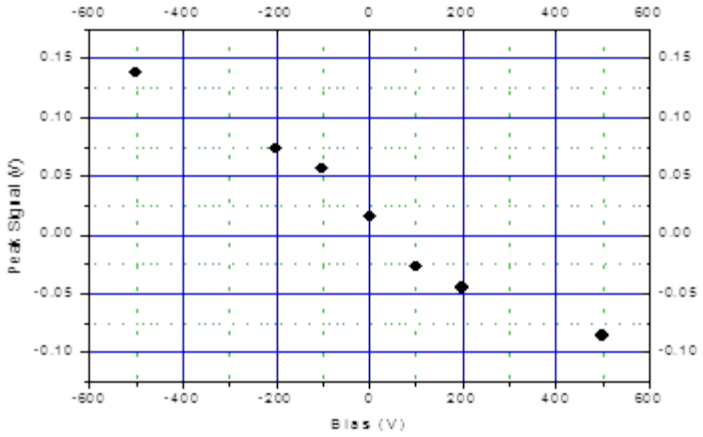

Figure 16. Results of linac shots 240-252 for glass microballoon (GMB)

3. EXPERIMENTAL APPARATUS AND TEST CHAMBER

Figure 17shows a view of the RIC test fixture for the glass microballon (GMB) dielectric before the dielectric sample and top electrode are assembled. Electrodes are present on either side of the sample when fully assembled. In Figure 18a view of the test cell in the assembly process is shown from a side perspective. Figure 19 shows an assembled view of a 10 lb. polyurethane foam sample with top electrode and guard ring.

The measured signals consist of prompt RIC, σ_p, and the delayed RIC, σ_d. The net current is the sum

$$I = Vd\left(\sigma_0 + \sigma_p + \sigma_d\right) + I_{dd}$$

where V is the bias, and d the sample thickness. The delayed conductivity may for some dielectric materials contain several terms with different decay constants, representing traps of different depths. In addition, there is a direct drive current I_{dd} produced by the electron beam. In the absence of bias the direct drive current can be determined, and the direct drive current can be a substantial part of the total RIC response when under bias. It can be difficult to determine the contribution of the prompt RIC for some polymers; however, for polyurethane foam the direct drive was not significant compared to the prompt and delayed conductivity contributions. For GMB, the samples acted more like solid dielectrics, and the direct drive was a significant portion of the signal that was measured.

The test chamber that housed the RIC (radiation induced conductivity) cell was evacuated to about 2E-4 Torr to eliminate any effects due to air/gas ionization near the circuit board, test fixture, and electrical connections. Of course the RIC response

within the gases contained within the closed cells of the foam were not affected by the vacuum, and these cells became highly conductive during the radiation pulse.

Radiation entered the test chamber through a collimated aperture. The aperture was smaller in diameter than the dielectric samples, assuring that only the central area of the dielectric was struck by radiation and that guard rings were not struck by the radiation. The vacuum test chamber is shown in Figure 20.

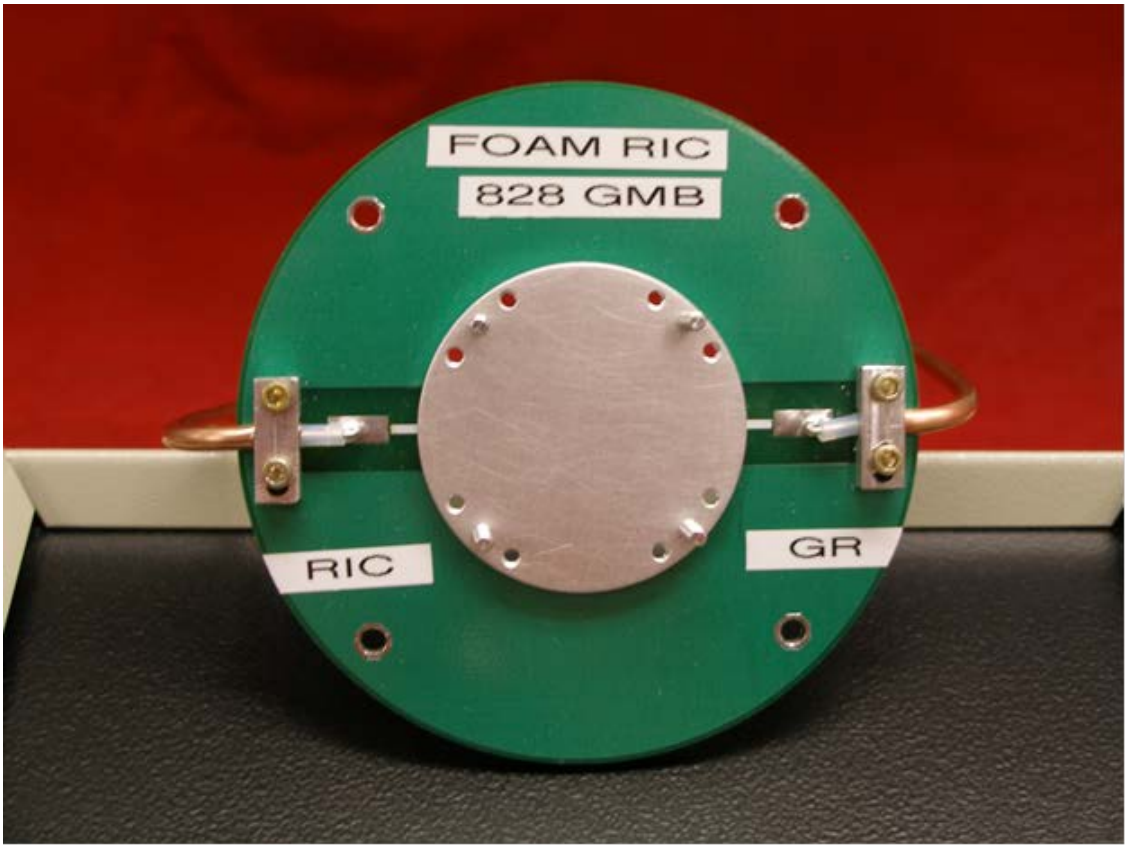

Figure 17. The base ground plane of the GMB assembly is shown before addition of GMB material

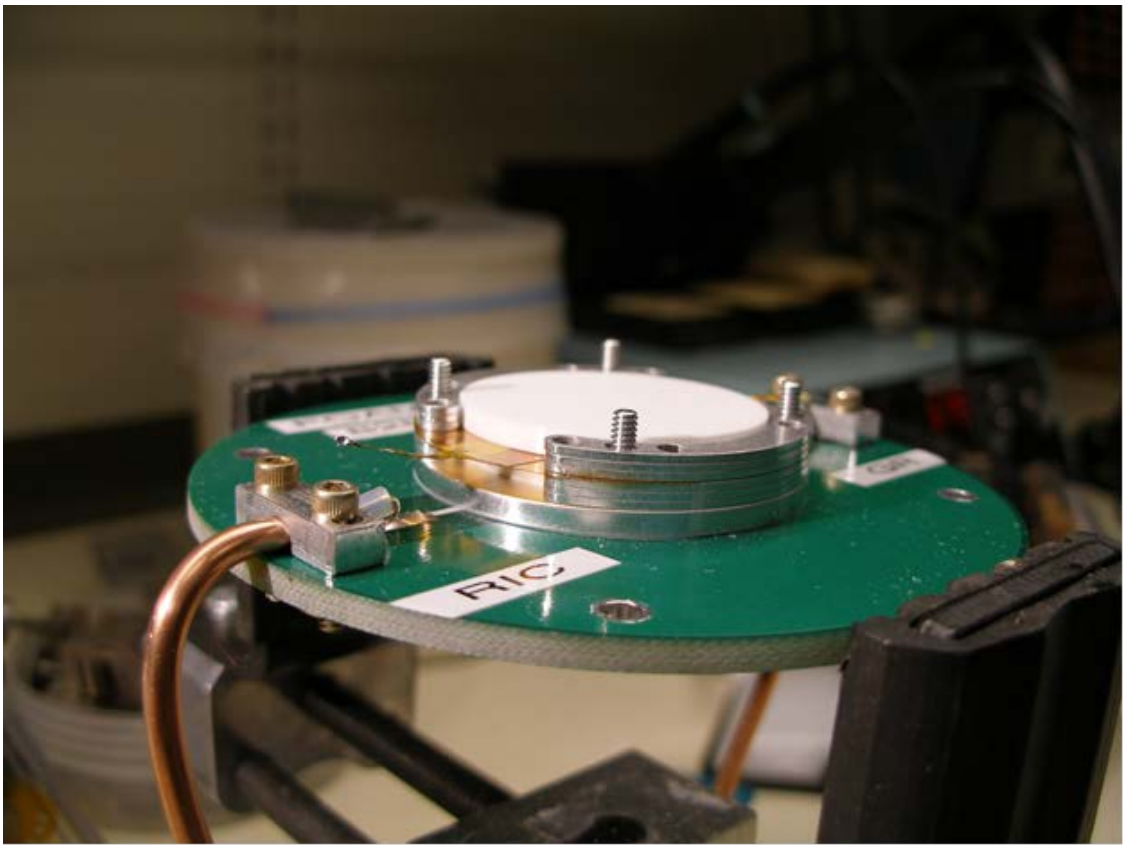

Figure 18. An in-assembly view of the GMB foam sample on ground plane

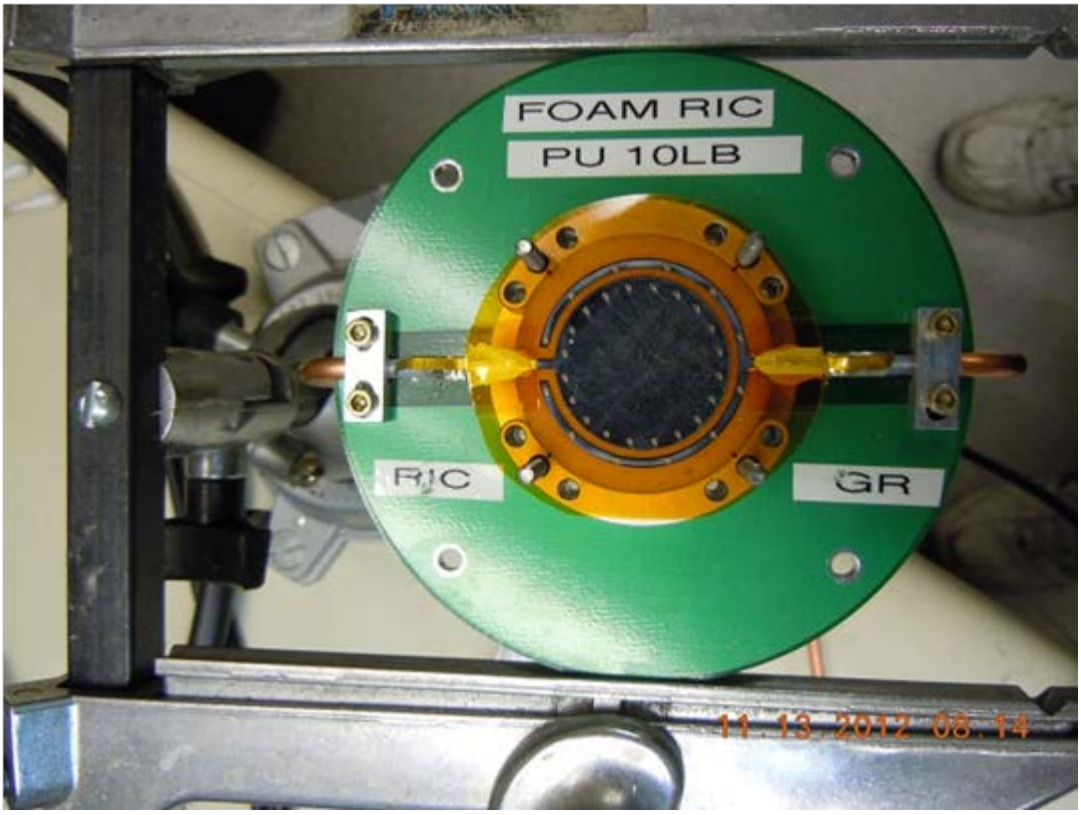

Figure 19. An assembled polyurethane 10 lb. foam sample with top electrode and guard ring

Figure 20. The vacuum test chamber showing aperture allowing radiation exposure of samples

4. ELECTRON BEAM CHARACTERISTICS

If a radiation source is not capable of providing consistent or repeatable output, including its spectrum, pulse width, and fluence, then the difficulty of performing repeatable and interpretable experiments is greatly magnified. We chose the Medusa LINAC at the Little Mountain Test Facility (LMTF) because it is capable of producing repeatable and predictable radiation output over long periods of time (such as reproducible pulsing over a week of experiments). We found through repeated testing that our dosimetry set consisting of silicon calorimeter, PIN diode, and PCD diamond detectors gave consistent repeatable readings shot-to-shot for the same conditions such as fixed distance from the source and fixed pulse width. The variation at the same conditions was approximately 1% shot to shot.

The nominal electron energy for the LINAC is 20 MeV, and the radiation pulse can be varied from 10 ns to 50 μs. For these experiments on foam samples, the radiation pulse width was about 50 ns FWHM. The dose rate range for these experiments was about 1E9 to 1E11 rad(Si)/s. For electron beam dosimetry, silicon calorimeters were supplemented with TLDs, PIN diodes, and PCDs. Measurement accuracy at the LINAC, including dosimetry and recording instruments, is estimated to be about 10%. For a more complete discussion and description of the linac radiation source and dosimetry accuracy see pages 11-17 of reference 2. An even more in depth discussion of the linac dosimetry techniques we employ and the accuracy of these measurements is provided in reference 12.

5. SUMMARY

We performed measurements and analyses of the prompt radiation-induced conductivity (RIC) in samples of polyurethane foam and glass microballoon foam at the Little Mountain Medusa LINAC facility in Ogden, UT. The polyurethane foam was closed cell and it exhibited strong charge trapping during the experimental series, so we had to remove the trapped charge for each measurement condition and only use the first shot in each series for the RIC analysis. The RIC coefficient was non-linear with dose rate for polyurethane foam; however, typical values at 1E11 rad(si)/s dose rate that were measured were 0.8E-11 mho/m/rad/s for 5 lb./cu ft. foam and 0.3E-11 mho/m/rad/s for 10 lb./cu ft. density polyurethane foam.

For encapsulated glass microballoons (GMB), this material acted more like a solid and did not build up much trapped charge. The measured RIC coefficient was approximately 1E-15 mho/m/rad/s and was not a strong function of dose rate.

6. REFERENCES

1. Mellinger, “Breakdown Threshold of Dielectric Barrier Discharge in Ferroelectrets”, IEEE Trans. on Dielectric and Electrical Insulation, Vol 18, Issue 1
2. E.F. Hartman, T. A. Zarick, T. J Sheridan, E.F. Preston, T. A. Stringer “Measurement of Prompt Radiation Induced Conductivity of Kapton”, SAND2010-7284, October 2010
3. Thomas J. Ahrenst and Frederick Wooten, "Electrical Conductivity Induced in Insulators by Pulsed Radiation," Nuclear Science, IEEE Transactions on, vol. 23, pp. 1268-1272, 1976.
4. J. F. Fowler, "X-Ray Induced Conductivity in Insulating Materials," Proceedings of the Royal Society of London A, vol. 236, pp. 464-480, 1956.
5. E F Hartman, T A Zarick, T J Sheridan, and E F Preston, “Measurements of Prompt Radiation Induced Conductivity of Teflon (PTFE)”, SAND2013-3714, May 2013
6. E. F. Hartman, "Measurements of Prompt Radiation Induced Conductivity of Fiberglass," Sandia National Laboratories Report SAND2010-2080 Sandia National Laboratories, 2010.
7. F Hartman, T A Zarick, M L McLain, T J Sheridan, E F Preston and T A Stringer, “Measurements of Prompt Radiation-Induced Conductivity of Pyralux”, SAND2013-10779, January 2014
8. M L McLain, F Hartman, T A Zarick, H P Hjalmarson, J D Gleason, K McDonald and T J Sheridan, “Effects of High Dose Rate Ionizing Radiation on Fused Silica and Sapphire Films”, IEEE Trans. on Nucl. Sci., Vol. 60, No.6, December 2013
9. M L McLain, E F Hartman, H P Hjalmarson, and G R Chanter, “Laser-Based Radiation-Induced Conductivity in Kapton Polymide Dielectrics at High Dose Rates”, JRERE, Vol.31,No. 1, July 2013
10. J H Simpson, “The Time Delay in Conduction and Breakdown Processes in Amorphous Solids”, Proc. Of Physical Soc., Sec. A, Vol. 63, 1050.

11. T A Stringer, M Burt, K J Dudley, W P Ballard, and D E Beutler, “SPHINX Measurements of Radiation Induced Conductivity in Foam” Abstract of paper for the 1999 HEART Conference, September 1998.

12. V. J. Harper-Slaboszewicz, E. Frederick Hartman, Marty R. Shaneyfelt, James R. Schwank, and Timothy J. Sheridan, "Dosimetry Experiments at the Medusa Facility (Little Mountain)," Sandia National Laboratories Report, SAND2010-6771, Sandia National Laboratories, 2010.

7. DISTRIBUTION

1 MS 245	S. C. Jones	0417
1 MS 245	D. M. Fordham	0417
1 MS 0344	J. M. Schare	02626
1 MS 0350	C. R. Landry	02133
1 MS 0405	M. Caldwell	0434
1 MS 0472	T. S. Edwards	02134
1 MS 0472	D L Thomas	02136
1 MS 1152	K. Cartwright	01352
1 MS 1152	C.D. Turner	01352
1 MS 1152	T. D. Pointon	01352
1 MS 1159	J.W. Bryson	01344
1 MS 1159	D. G. Talley	01344
1 MS 1159	K.J. McDonald	01344
1 MS 1159	G. S. Heffelfinger	01340
5 MS 1167	E.F. Hartman	01343
1 MS 1167	T.A. Zarick	01343
1 MS 1167	T.J. Sheridan	01343
1 MS 1167	T.M. Flanagan	01343
1 MS 1167	M.L McLain	01343
1 MS 1168	L. X. Schneider	01350
1 MS 1168	B. V. Oliver	01352
1 MS 1178	M.L. Kiefer	01656
1 MS 1179	L. Lorence	01341
1 MS 1179	C.R. Drumm	01341
1 MS 1179	W. C. Fan	01341
1 MS 1179	H.P. Hjalmarson	01341

1 MS 0899	Technical Library	9536 (electronic copy)


Sandia National Laboratories